CANCOM2024 – CANADIAN INTERNATIONAL CONFERENCE ON COMPOSITE MATERIALS

# DYNAMIC AXIAL CRUSHING OF UD-NCF COMPOSITE CLOSED CHANNELS FOR CRASHWORTHINESS APPLICATIONS

Ajayi, Valerie Atinuke Oluwapelumi[1], Worswick, M[1], Montesano, J[1]*
[1] Mechanical and Mechatronics Engineering, University of Waterloo, Waterloo, Canada
* Corresponding author (john.montesano@uwaterloo.ca)

**Keywords**: *non-crimp fabric composites, crashworthiness, dynamic loading*

## ABSTRACT

This contribution summarizes an experimental investigation into the energy-absorbing capabilities of closed-channel unidirectional non-crimp fabric carbon fiber-reinforced epoxy laminates manufactured via high-pressure resin transfer molding. Two stacking sequences of eight-ply channels with hat-shaped cross-sections were manufactured: $[0/\pm45/90]_s$ and $[\pm45/0_2]_s$. Pairs of channels are bonded together with a structural adhesive and impacted with an 855kg sled at 7.5 m/s. Dynamic axial loading of closed channel components provides experimental data to investigate the progressive crushing behaviour of CFRP channels for applications in vehicle deceleration under high-strain rates.

Three impact tests were performed for each bonded closed-channel specimen configuration. The results revealed that specimens comprising of channels with the stiffer stacking sequence ($[\pm45/0_2]_s$), exhibit a higher average mean crush force (32%), higher average peak force (30%), and higher specific energy absorption per kilogram (32%). Additionally, none of the tested specimens failed as a result of crack propagation through the adhesive or via debonding. However, in comparison to the performance of the tested unbonded channels with the same stacking sequence and cross-section, the closed-channel specimens exhibited reduced specific energy absorption for both stacking sequences (30%), and thus underperformed in terms of mean crush force as well. Causes of this underperformance can be attributed to misalignment between one channel with respect to another within a bonded pair, the quality of the channels, and the difference in crush distance between the two sets of tests which add difficulty in directly comparing the results. Additionally, while brittle fracture is the predominant failure mode of the open (unbonded) $[\pm45/0_2]_s$ channels, splaying is the predominant failure mode of the $[\pm45/0_2]_s$ closed-channel specimen. Lastly, these results serve as data to validate future predictions of failure mode and energy absorption generated via finite element models.

# 1 INTRODUCTION

While the potential of carbon fibre-reinforced plastic (CFRP) composites for energy absorption and structural applications has been widely acknowledged, there has been limited adoption in the automotive industry due to the costs associated with manufacturing CFRP composites and the difficulty in predicting the performance of such structures. CFRPs absorb energy through a complex interaction of damage mechanisms (i.e., matrix cracking, fibre/matrix debonding, fibre pull-out, kinking or fracture, delamination and inter/intralaminar friction [1]) that are difficult to predict and quantify. Additionally, performance is heavily dependent on geometry, fibre properties, stacking sequence, and damage initiation strategies.

Rapid liquid composite molding processes with highly reactive resins and unidirectional non-crimp fabric (UD-NCF) reinforcements may enable further adoption of CFRP composites as energy-absorbing parts for the high-volume production of vehicles. Components made via high-pressure resin transfer molding (HP-RTM) offer reduced cycle times (as low as 2 minutes per part) [2], while UD-NCF reinforcements provide a reduction in manufacturing cost, ease of handling, and strength [3]. This enables them to be readily adopted into high-volume manufacturing instead of more traditional carbon fibre fabrics. Additionally, they increase lightweighting potential as a result of the flexibility offered in tailoring material anisotropic properties and part performance.

The energy absorption characteristics of NCF composites have not been widely studied, and of the available literature, many focus on quasi-static axial crushing or dynamic drop-testing. In this study, CFRP channels are bonded together with structural adhesive, 3M 07333, and tested via dynamic axial loading. Their performance is evaluated and compared to the behavior observed for open channels of similar geometry.

# 2 METHODOLOGY

## *2.1 Materials & Geometry*

Open/single hat channels as shown in Figure 1 were manufactured at the Fraunhofer Innovation Platform for Composites Research (FIP–Composites) at Western University via high-pressure resin transfer molding (HP-RTM). The material system consists of unidirectional non-crimp carbon fibre (ZOLTEK™ PX35 UD300 UD-NCF) and a snap-cure resin epoxy matrix (HEXION EPIKOTE™ TRAC 06150) [4]. Two stacking sequences were manufactured and considered in this study: $[0/\pm45/90]_s$ and $[\pm45/O_2]_s$. The average thickness of the channels was 2.6 mm [4]. The properties of the cured ply, which averaged 53% volume fraction, are summarized in Table 1 below [5].

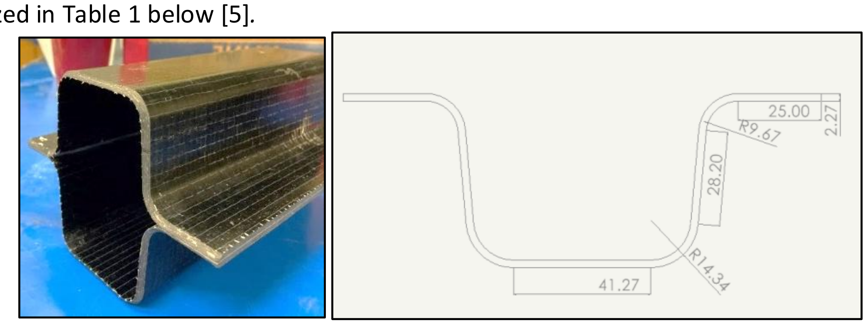


*Figure 1: (a) Fabricated closed channel and (b) cross-sectional geometry of hat channel.*

*Table 1: Ply properties of UD-NC ply, 53% volume fraction [5].*

| Mechanical Properties | | | |
|---|---|---|---|
| Density [g/cm^3] | 1.46 | Transverse Compressive Strength, $Y_c$, [MPa] | 145 (±4) |
| Longitudinal Young's Modulus, $E_1$, [GPa] | 121 (±7) | In-Place Shear Strength, $S_L$, [MPa] | 90 (±2) |
| Transverse Young's Modulus, $E_2$, [GPa] | 8 (±2) | Fibre Longitudinal Strain at Failure $\varepsilon_{1f\%}$ [%] | 0.66 (±0.07) |
| Major In-Plane Poisson's Ratio, $v_{12}$ | 0.37 (±0.01) | Fibre Transverse strain at failure $\varepsilon_{2f}$ [%] | 0.66 (± 0.07) |
| In-Plane Shear Modulus, $G_{12}$ [GPa] | 3.55 (± 0.14) | Composite Longitudinal Strain at Failure $\varepsilon_{1c}$ [%] | 0.8 (± 0.09) |

| | | | |
|---|---|---|---|
| Longitudinal Tensile Strength, $X_t$, [MPa] | 1637 (±168) | Composite Transverse Strain at Failure $\varepsilon_{2c}$ [%] | 2.42 (±0.33) |
| Transverse Tensile Strength, $Y_t$, [MPa] | 60 (±4) | In-Plane Shear Strain at Failure $\gamma_{12}$ [%] | 8.88 (±1.9) |
| Longitudinal Compressive Strength, $X_c$, [MPa] | 1001 (±97) | | |

### 2.2 Sample Preparation (Bonding)

Pairs of open channels, originally 800 mm long, were bonded together to form one closed channel using the structural adhesive, 3M 07333. Prior to bonding, the flanges of each channel were cleaned with acetone and then sanded until an approximate surface roughness of 0.75 ($R_a$) was achieved along the length of each flange. After the surfaces were once again cleaned with acetone, the adhesive was applied and cured according to operational instructions (30 minutes at 80°C) (Figure 2(a)). A target bond line thickness of 0.65 millimeters was set to maximize the strength of the bond and avoid failure through the adhesive. Increases in bond strength up to 0.65mm were demonstrated in [6] and a similar methodology for bonding was undertaken.

To maintain a 0.65 mm bond line thickness across the channels, 0.65 mm shims were manufactured (Figure 2(b)) and treated with LOCTITE FREKOTE mold release as per operational instructions. Each channel included extra flange width that required trimming to align with the designed geometry (Figure 1(b)). The shims were adhered to this extra width to guide the bond line thickness and trimmed after curing. Fixtures with the envelope of the outside surface of the channels were 3D printed and attached to the channels to improve the alignment of one channel with respect to the other (Figure 2(c)) after the initial trials. These fixtures were also treated with a mold release agent and placed intermittently along the length of the channels. C-Clamps were then added around the fixture to maintain the aligned orientation.

After curing, the shims and excess flange width on each side of the channels were trimmed using a diamond Rubi saw to achieve the desired cross-section. The channels were also cut to approximately 200 mm in length. Lastly, a 45° chamfer 2.5mm in thickness was machined at one end of the channel to serve as a progressive crushing initiator. The other end of the channel was leveled to ensure the component was square. An example of a completed closed channel is displayed in Figure 2(d).

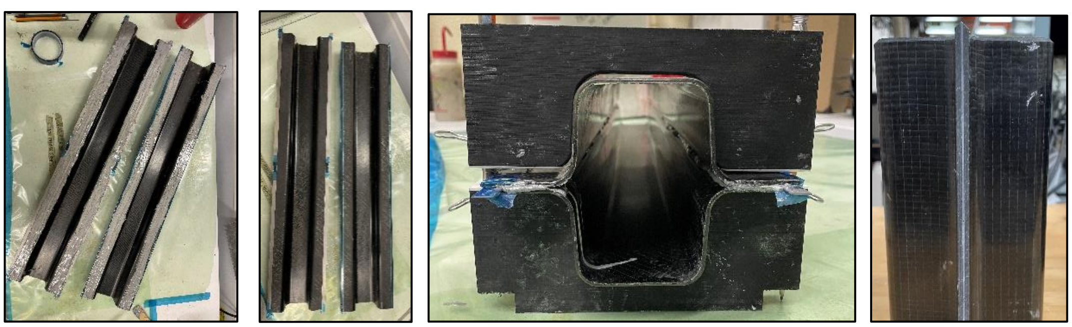

*Figure 2: (a) Adhesive applied to flanges of channels, (b) shims attached to channels, (c) printed fixtures for alignment, and (d) cured sample.*

### 2.3 Experimental Set-Up

Experimental testing was performed using the experimental set-up shown in Figure 3(a). An 855kg sled was translated in the axial direction of the channels at a speed of 7.5 m/s for approximately 90 mm of free crush distance. The bottom 50 mm of the channel was secured to a wall using the fixtures shown in Figure 3(b). Aluminum honeycomb decelerators were attached to either side of the channel to stop the sled after achieving the desired crush distance. Data was captured at a frequency of 10,000 Hertz and each test was approximately 30 milliseconds. High-speed cameras (10,000 frames per second) were placed on either side of the channel to capture deformation along the bonded flanges. Lastly, a glass enclosure was set around the experiment with inserts for vacuums to capture dust.

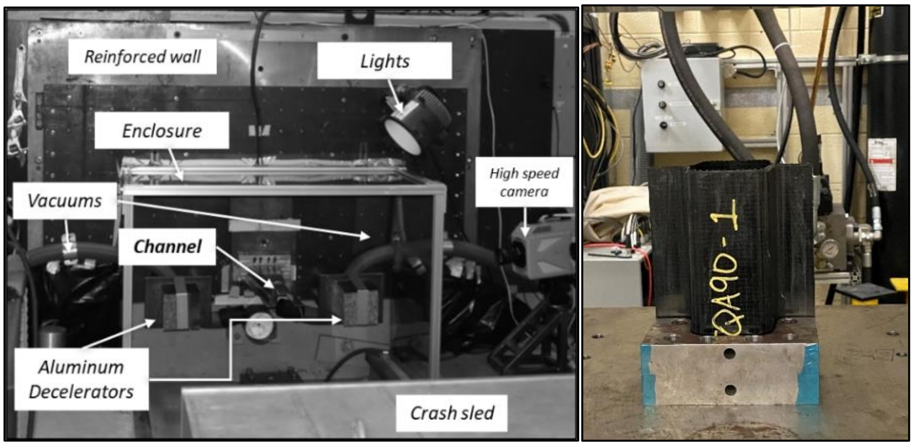


*Figure 3: (a) Experimental set-up for dynamic axial loading of closed hat channels and (b) fixtures to secure channel.*

## 3 Results & Discussion

The average force-displacement response and energy absorption under dynamic loading of three trials per stacking sequence is shown below in Figure 4. The individual trials are also included in grey. The peak forces, mean crush forces, and energy absorption are summarized in Table 3. The $[\pm45/0_2]_s$ channels exhibited an average 30% higher mean crush force than the $[0/\pm45/90]_s$ channels. Similarly, the average peak force of the $[\pm45/0_2]_s$ hat channels was greater than the $[0/\pm45/90]_s$ channels by about 32%. Lastly, the specific energy absorption (SEA, energy absorption per mass) of the $[\pm45/0_2]_s$ channels was 32% greater than the $[0/\pm45/90]_s$ channels. This can be compared to the performance of the open channels where the $[\pm45/0_2]_s$ open channels displayed 38% higher specific energy absorption than the $[0/\pm45/90]_s$ open channels [4].

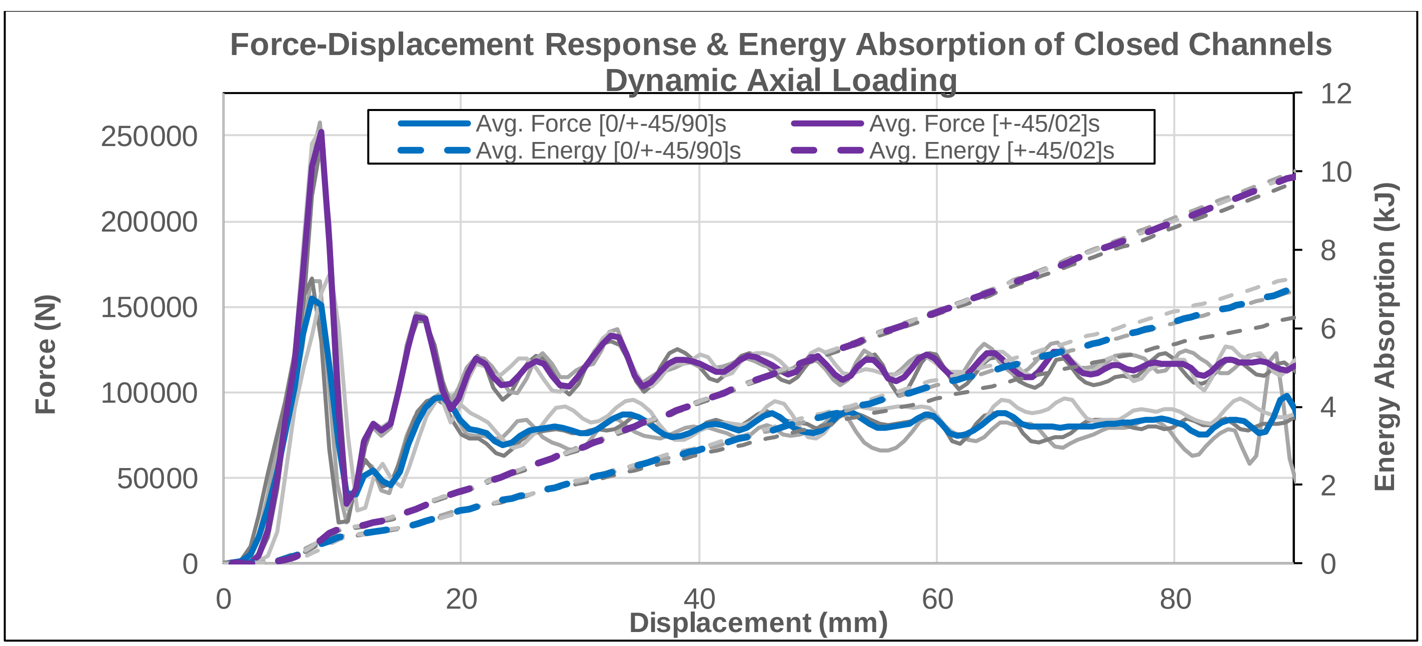


*Figure 4. Force-displacement responses and energy absorption of closed hat channels under dynamic axial loading.*

*Table 3. Summary of Performance of Closed Hat Channel Under Dynamic Axial Loading.*

| | $[0/\pm45/90]_s$ Channel | $[\pm45/0_2]_s$ Channel |
|---|---|---|
| **Peak Force (kN)** | 167.4 ± 2.5 | 246.3 ± 4.8 |
| **Mean Crush Force (kN)** | 76.0 ± 4.8 | 107.9 ± 1.4 |
| **Specific Energy Absorption (kJ/g)** | 36.2 ± 1.4 | 53.8 ± 1.6 |
| **Notable Failure Modes** | Brittle Fracture & Fragmentation | Brittle Fracture & Splaying |

The average mean crush force of the open $[\pm45/0_2]_s$ channels was 73.3 kN and the average mean crush force of the $[0/\pm45/90]_s$ open channels was 40.0 kN [5]. Thus, the closed $[0/\pm45/90]_s$ channels average a mean crush force almost double the open channels, which is to be expected. However, there is only a 30% increase in the mean crush force of the closed $[\pm45/0_2]_s$ channels in comparison to the open $[\pm45/0_2]_s$ channels. While there was an observable decrease in the quality of the channels used for the closed channel testing in comparison to the open channels (i.e. waviness, some dry fiber, etc.), the consistency of the force-displacement results suggests that defects did not significantly affect the performance from one channel to another. Next, one may consider the misalignment of one channel with respect to the other when bonding two channels together. This may have had a more pronounced effect in the $[\pm45/0_2]_s$ channels where there are more 0-degree piles, as opposed to the $[0/\pm45/90]_s$ channels. Lastly, the figures provided by Harvey et al. [4] suggest significantly more brittle fracture in the open $[\pm45/0_2]_s$ channels whereas there are more fronds and relative mass remaining in the closed $[\pm45/0_2]_s$ channels (Figure 5).

Figure 5 shows examples of the crushed closed $[\pm45/0_2]_s$ and $[0/\pm45/90]_s$ channels. As mentioned, it can be seen that there are more layers/fronds remaining in the $[\pm45/0_2]_s$ channel than in a channel where brittle fracture is the predominant failure mode. This remaining material, which suggests less dissipation of energy through crushing, may motivate the reduced mean crush force of the $[\pm45/0_2]_s$ channels and thus, the reduced final specific energy absorption of 53.8 kJ/g (30% less than the comparative open channel). Additionally, despite the $[0/\pm45/90]_s$ open channels performing as expected (average mean crush force twice the open channel), it also exhibits a reduced SEA (25% less than open channels). The failure mode of the closed $[0/\pm45/90]_s$ channels remain the same as the $[0/\pm45/90]_s$ open channels: fragmentation. A contributing factor to the reduced SEA may be the shorter free crush distance for both channels (90 mm versus 200 mm). Since progressive crushing is propagated through the formation and growth of a debris wedge, increased crushing distance means that there is a large debris wedge with more material in the center of the channel. This material provides additional support to the structure under compressive loading and thus, may improve energy absorption under compaction. Thus, SEA calculated up to 90 mm for the open channels may provide more comparative values. Lastly, as can be seen in Figure 5, failure does not occur at or near the adhesive, suggesting the structural adhesive is sufficient for axial crushing applications.

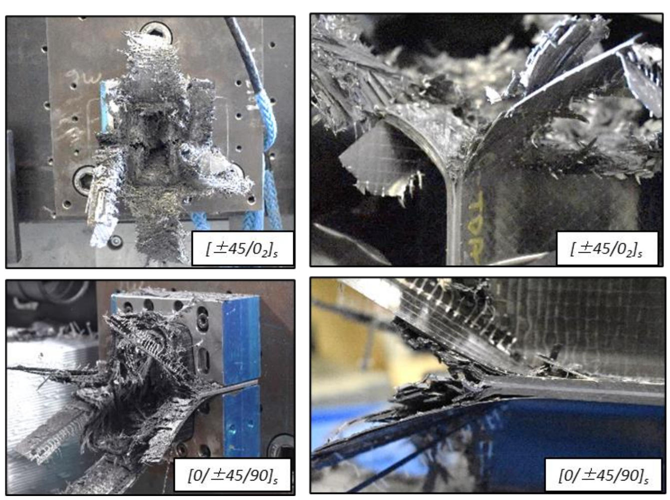


*Figure 5: Crushed closed hat channels displaying splaying/lamina bending ($[\pm45/0_2]_s$) and fragmentation ($[0/\pm45/90]_s$).*

# 4 Conclusion

For energy-absorbing applications, it must be certified that carbon fibre reinforced polymers (CFRP) structures can provide sufficient levels of crashworthiness to ensure passenger safety. This study investigated the performance of closed channels under dynamic axial loading for application in vehicle deceleration to protect occupants. As is seen in the case of open channel loading, the stiffer closed channels ($[\pm45/0_2]_s$) perform better than the closed $[0/\pm45/90]_s$ *channels* in terms of energy absorption (by 32%), mean crush force (by 32%), and peak force (by 30%). Whereas the latter stacking sequence dissipates energy predominantly through fragmentation, the former exhibits more splaying/lamina bending where friction is able to absorb more energy [8]. The force-displacement responses of both stacking sequences are consistent across trials, indicating a successful bonding method. In comparison to the open channels, the closed channels do not show significant improvement in SEA, and a different predominant failure mode is seen in the closed $[\pm45/0_2]_s$ channels (splaying).

Limitations

In terms of limitations, there were many opportunities for the introduction of human error during the bonding process. More specifically, the alignment of channels to one another, the manufacturing of the triggers, and the final width of the flanges were all completed manually, and variations are expected in all three of these geometric constraints from one closed channel to another. Similarly, the bond line is thick such that it is difficult to ensure consistency across the width of the flange, and the quality of the bond line toward the center of the channel was not measured.

Future Work

Having completed dynamic axial testing, quasi-static axial crushing of the closed channels would provide further insight into the performance of the closed channels and energy-dissipating mechanisms. Based on the open channels results, the $[\pm45/0_2]_s$ channels are expected to outperform the $[0/\pm45/90]_s$ channels through significant splaying of bundles of fibers. Additionally, the experimental data gathered in this study may be used to validate models predicting the performance of UD-NCF channels.

# 5 REFERENCES

[1] B. G. Falzon, "Computational modelling of the crushing of carbon fibre-reinforced polymer composites," *Philosophical Transactions: Mathematical, Physical and Engineering Sciences,* 2022.

[2] “High-pressure resin transfer molding,” *Huntsman Transportation*, 17-May-2022. [Online].

[3] S. V. Lomov, Non-crimp fabric composites: Manufacturing, properties, and applications. Oxford: Woodhead, 2011

[4] Harvey B, Ghazimoradi M, Worswick MJ, Montesano J. Energy absorption of carbon fiber reinforced plastic channels under dynamic axial crush loading. *SPE Automotive Composites Conference & Exhibition (ACCE)*, Novi, US, Nov 2-4, 2021.

[5] A. P.Suratkar, “Damage in Non-Crimp Fabric carbon fiber reinforced epoxy composites under various mechanical loading conditions,” Ph.D. dissertation, Mechanical and Materials Engineering, University of Western, London, Ontario, 2022.

[6] R. C. Dehaghani, “Experimental and Numerical Assessment of Adhesively Bonded Non-Crimp Fabric Carbon Fiber/Epoxy Composite Joints,” Masc. thesis, Mechanical and Mechatronic Engineering, University of Waterloo, Waterloo, Ontario, 2021.

[7] J. M. Starbuck, D. O. Adams and M. Courteau, "Energy Absorbing Damage Mechanisms in Progressive Crushing of Composite Tubes," *32nd American Society of Composites Technical Conference*, 2017.